J. Fluid Mech. (1966), *vol.* 25, *part* 4, *pp.* 795–816
Printed in Great Britain

The directional spectrum of ocean waves: an experimental investigation of certain predictions of the Miles–Phillips theory of wave generation

By A. W. R. GILCHRIST†
Institute of Oceanography, University of British Columbia

(Received 4 November 1965)

The directional spectrum of wind-driven surface waves has been measured under conditions of limited fetch, in order to check the predictions of the Phillips–Miles theory of wave generation (Miles 1960). The expression obtained for the directional spectrum in this theory involves the spectrum of the atmospheric pressure fluctuations, but it is possible to obtain theoretical estimates of the major features of the directional spectrum without knowledge of the pressures. Specifically, it is possible to predict the frequency at which the power spectrum should peak, and, for the higher frequencies, the range of azimuth over which high spectral values should be observed; for the lower frequencies the theory indicates a bimodal distribution in azimuth (Phillips's resonance wavês), and gives the angle of travel relative to the wind as a function of frequency.

The results of the measurements are in fairly good agreement with the theoretical predictions for the higher frequencies. The asymmetry of the fetch results in the prediction that the waves will travel at an angle to the wind which varies with frequency, and this was observed. The range of azimuth over which the spectral density is high is also close to the theoretical prediction. For the low frequencies the bimodal distribution was not observed: the waves were found to have a single predominant direction of travel at each frequency. However, this direction conformed closely to that of one of the two wave trains predicted by Phillips, and its variation with frequency was also that given by the theory. There is reason to suppose that the peculiarities of the experimental site may be responsible for the absence of the second wave train, especially as it would be difficult to account for the observed effects on any basis other than that of Phillips's theory.

1. Introduction

In an article reviewing the status of our knowledge of the process of wave generation, Ursell (1956) remarked that three elements were necessary: a correctly derived theory, a body of relevant measurements, and a demonstration of agreement between the two; he added that at that time all three were lacking. The theories of Phillips (1957) and Miles (1957), as combined by Miles (1960), have

† Now at: Defence Research Telecommunications Establishment, Defence Research Board, Ottawa, Canada.

since provided the first of these elements, but Kinsman (1965) has pointed out that the other two are still awaited. A full verification of the theory would require the measurement of the two-dimensional spectrum of the pressure fluctuations in the atmosphere, simultaneously with that of the water surface elevation. The former has never been measured, and appears to present considerable difficulties. However, the major predictions of the theory can be investigated using measurements of the directional spectrum of the surface elevations alone. The latter has been measured only a few times, and then under conditions which do not provide an adequate check of the theory. In particular, the physical existence of Phillips's resonance waves remains to be demonstrated.

The measurements reported here were conducted in a small coastal inlet, in which the fetch was well defined over most of the azimuth, and with moderate wind speeds so that the sea was only partially developed. These conditions are such that a discriminating test of the theory is possible. While in the prior investigations resonance waves had to be sought as residual traces under conditions where their characteristic features were swamped through the action of Miles's mechanism, it was anticipated that in the present case waves of measurable amplitude should exist over a range of frequencies in which the Miles mechanism had not become operative; these should be pure resonance waves, according to the theory. Measurements made under these conditions therefore appeared to offer the possibility of a positive demonstration of the existence of resonance waves. For the higher frequencies, at which the Miles mechanism should be acting, definite predictions could be made for the direction of travel and angular spread of the waves, so that a critical test was possible in this régime also.

2. Theory

2.1. *The Phillips–Miles spectrum: method for predicting characteristics of spectrum*

The end result of the unified Phillips–Miles theory is an expression for the directional spectrum of the surface displacement. This expression as given by Phillips & Katz (1961) is:

$$\phi(\mathbf{k},t) = \frac{f(t,m)}{2\rho^2 c^2}\int_0^\infty \Pi(\mathbf{k},\tau)\cos\omega\tau\, d\tau, \tag{1}$$

where $\phi(\mathbf{k},t)$ is the directional spectrum, $\mathbf{k}$ the vector wave-number, t the time from the onset of the wind, ρ the water density, c the wave phase speed, ω the wave angular frequency, $\Pi(\mathbf{k},\tau)$ the time-lagged spectrum of the turbulent atmospheric pressure fluctuations, i.e. the spatial Fourier transform of the covariance between pressures at points of the surface separated by a distance $\mathbf{r}$ and time τ,

$$\begin{aligned} f(t,m) &= (e^{2mt}-1)\,(2m)^{-1} \\ &= t[1+mt+O\{(mt)^2\}], \\ m &= \tfrac{1}{2}\zeta kc, \end{aligned}$$

and ζ is the fractional increase in wave energy per radian; its evaluation requires the solution of the Orr–Sommerfeld equation. A solution has been obtained by Conte & Miles (1959) for the case of a logarithmic wind-velocity profile.

Although no measurements of the pressure spectrum have been made, some indirect evidence exists which suggests that

$$\frac{1}{c^2}\int_0^\infty \Pi(\mathbf{k},\tau)\cos\omega\tau\,d\tau$$

is a unimodal function, approaching zero for both large and small wave-numbers, and with a fairly broad maximum in the range of wave-numbers around $k = 10^{-2}\,\mathrm{cm}^{-1}$ (Phillips 1957). This evidence therefore suggests that the unknown part of the expression for $\phi(\mathbf{k},t)$ may be assumed to vary only slowly over the range of wave-numbers of interest in the present investigation. The directional spectrum is then dominated by the exponential factor $f(t,m)$.

Considering the series expansion for $f(t,m)$, it is apparent that, for $mt \ll 1$, $\phi(\mathbf{k},t)$ increases linearly with the wind duration t, as is characteristic of Phillips's mechanism; the expression for $\phi(\mathbf{k},t)$ then in fact reduces to that derived by Phillips. For fixed k (or m) the rate of growth increases with increase in t and eventually exhibits the exponential variation typical of Miles's process. The transition from one mechanism to the other may be assumed to occur when $mt \sim 1$, i.e. at a wind duration

$$t_T(\mathbf{k}) = m^{-1} = (\tfrac{1}{2}\zeta kc)^{-1}. \tag{2}$$

Now in the present investigation the waves are limited by fetch rather than by the duration of the wind. The relation between fetch and duration is $F = c_g t$, where c_g is the group velocity of the waves (Phillips 1958*a*). The above expression for the wind duration necessary to produce transition can therefore be written in terms of fetch as $F_T(\mathbf{k}) = (\zeta k)^{-1}$; if fetch is measured in wavelengths we obtain

$$\{F_T(\mathbf{k})/\lambda_T\} = (2\pi\zeta)^{-1}, \tag{3}$$

which is a function of c/U and α, the angle between the directions of the wind and wave propagation; the quantity U is the wind speed. In order to apply this result, the numerical values of ζ calculated by Conte and Miles must be used.

Experimental wave power spectra are found to exhibit a characteristic variation with frequency: from low levels at low frequencies the density rises very rapidly to a maximum, and then falls off more slowly with further increase in frequency. Up to the stage at which the spectrum is no longer limited by fetch, i.e. until the sea is fully developed, it is found that the rapid rise in the spectrum occurs at lower frequencies as the fetch is increased. Considering the spectral density as a function of fetch for a fixed frequency, as the fetch increases the density at first increases slowly, and then rises rapidly to a much higher level; with further increase in fetch this higher level is maintained. But this is the behaviour we should expect to occur in the transition from the Phillips to the Miles mechanism, if we realize that the exponential growth of the latter must ultimately be limited by non-linear processes not taken into account in the theory. This suggests a correspondence between the theoretical transition frequency and the observable frequency of the rapid rise of the spectrum. A quantitative comparison has been made by Phillips & Katz (1961) using the experimental data of Burling (1959) and Kinsman (1960). The comparison

was actually made in terms of the transition fetch rather than the transition frequency for a given fetch, and a considerable amount of scatter was found in the data, although the observed fetches were certainly in order-of-magnitude agreement with the theoretical transition fetch. As will be seen in § 2.2 the transition fetch–frequency relation is such that the transition frequencies are much less variable. The preceding argument, including the derivation of the theoretical transition fetch, is due to Phillips & Katz (1961).

The above ideas may be applied to the directional spectrum also, since the transition fetch is a function of the vector wave-number. The indicated correspondence between the theoretical transition and the sharp rise of the power spectrum enables us in this case to predict ranges of azimuth for a given frequency over which high spectral values should be found; these are the ranges in which the Miles mechanism has become effective. At any frequency above that of the peak of the power spectrum (the Miles régime) this mechanism may be expected to dominate the directional spectrum, although the effect of energy transfers between wave modes (Phillips 1960) may produce a tendency towards isotropy—i.e. towards broadening the directional spectrum—at the higher frequencies.

For the low frequencies, such that transition does not occur at any azimuth, only Phillips's mechanism can be operative. Only forced waves and resonance waves should then be present, and the latter should dominate the directional spectrum. The theoretical prediction is particularly simple in this case: at any frequency there should exist two wave trains making angles of $\pm \cos^{-1}(c/U)$ with the wind direction. We do not, of course, expect to observe such sharply defined trains, if only because any physically realizable filter has a finite bandwidth. Neither do we expect sharply defined trains to exist in the water; the normal fluctuations in wind speed and direction would ensure some angular spread, and so too would the finite correlation times of the pattern of atmospheric pressure fluctuations. The actual prediction is that the spectral density will be high in two more or less narrow ranges of azimuth centred on the theoretical resonance angles.

If experimental conditions are such that c/U is close to unity at the peak of the power spectrum the sea is said to be fully developed. Since the Miles mechanism is very inefficient at frequencies such that $c/U \sim 1$, it might be thought that the waves at these frequencies would be mainly resonance waves. However the resonance angle is then zero, so that the resonance waves travel with the wind, as also do Miles waves in the open sea. Thus the two cannot be distinguished by their directional properties. At higher frequencies such that $c/U < 1$, resonance waves may be identified by their characteristic angles of travel, but in the fully developed sea the Miles mechanism has taken over at these frequencies, and so there is little hope of identifying them. However, under appropriate conditions of limited fetch and wind speed, which are easily derivable from the theoretical expression for the transition fetch, the power spectrum peaks at small values of c/U, and a decisive identification of the resonance waves should be possible. The present investigation was designed to achieve this.

Quantitative characteristics of the directional spectrum predicted by the theory for the conditions of this investigation are presented in § 2.2.

It should be noted that the theory presented above applies to waves in deep

water. The conditions of the experiment were such that limited depth effects become important only at low frequencies in the range considered. These effects are taken into account in the discussion of the results.

2.2. *Predicted characteristics of the spectrum for the conditions of the investigation*

2.2.1. *Experimental conditions*

(*a*) *Fetch.* The distance from the shore to the point of observation is called the fetch. This is shown in figure 1, which is a map of Burrard Inlet showing the

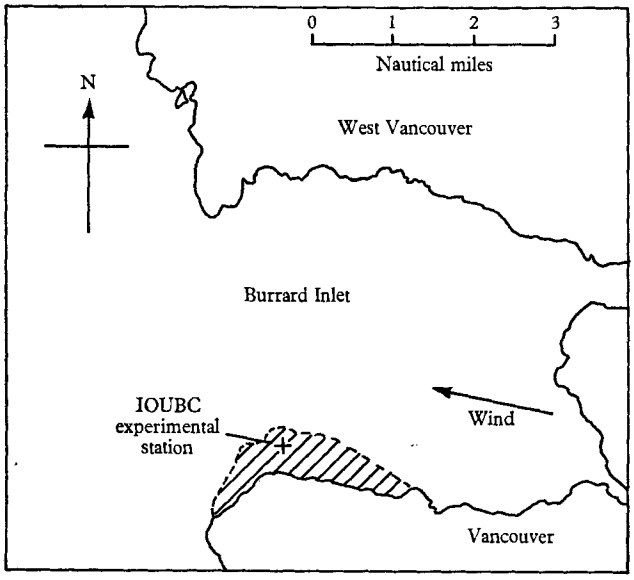

FIGURE 1. Map of experimental site.

coastline and the location of the Institute of Oceanography, University of British Columbia (IOUBC) oceanographic research station, where the measurements for this project were made. Figure 2 is derived from figure 1 and presents the fetch as a function of azimuth.

(*b*) *Wind.* For the set of measurements analysed in detail the mean wind direction was 102° true. This direction is indicated by an arrow in figure 1, and is the zero of the scale marked θ_{wind} in figure 2. The wind speed, measured at a height of 2 m above the water surface, was 5·8 m/sec. The measurement of wind speed and direction is discussed in § 3.

(*c*) *Array orientation.* The array of wave probes was arranged in a line running roughly north and south, actually 175°–355° true. In figure 2 the scale marked θ_{array} represents angles measured from an origin corresponding to 175° true; the sense of the angle θ_{array} follows the mathematical convention, which is opposite to the convention used for compass bearing.

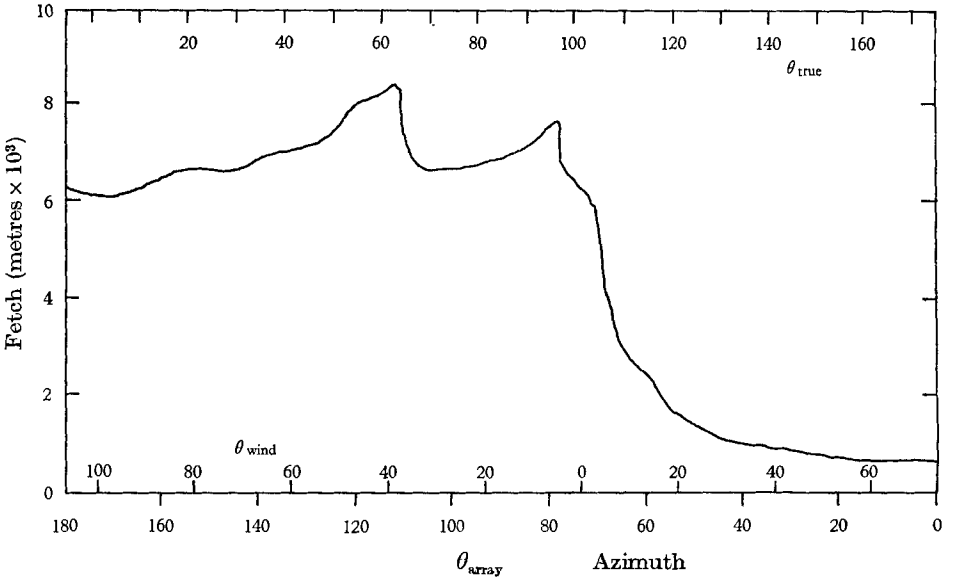

FIGURE 2. Fetch available at experimental site.

2.2.2. *The growth rate parameter*

As was pointed out in § 2.1 the evaluation of ζ, the fractional increase in wave energy per cycle, requires a knowledge of the wind profile. The values calculated by Conte & Miles apply to a logarithmic profile, which is the theoretical form for a turbulent boundary layer in an unstratified fluid. Measurements made over water (e.g. Hamblin 1965) occasionally give profiles of this form, but more often do not, even under neutral conditions.

According to Miles's theory the value of ζ is proportional to the profile curvature, so that even if the profile is close to logarithmic it is possible for the curvature to be significantly different. Benjamin (1959) has shown that different but not unreasonable profiles can lead to variations of the order of 50 % in the theoretical transition fetch. In their comparison of the measured transition fetch with theoretical predictions, Phillips & Katz found a scatter of this order of magnitude among the observations. This was presumably due, in part at least, to differences in the profile curvature. The theoretical fetch calculated by Phillips & Katz was based on a logarithmic profile:

$$U(z) = U_1 \log_e z/z_0, \tag{4}$$

in which the parameters U_1 and z_0 were given values typical of measured profiles at the wind speed concerned.

Because of the great difficulty of measuring profile curvature, and the virtual uselessness of ordinary profile measurements for this purpose, the theoretical predictions in this section are based on a logarithmic profile with parameters appropriate to the measured wind speed. Only order-of-magnitude agreement can be expected with these predictions, but this is in any case inherent in the analysis, which starts from the order-of-magnitude relation that transition will

occur when $mt \sim 1$. It is possible that the variation with frequency of the quantities concerned may be predicted more reliably than their absolute magnitude.

In the following estimates the profile parameters used are $U_1 = 0{\cdot}6$ m/sec and $z_0 = 0{\cdot}1$ mm. These values are derived from Hamblin's work and are similar to those obtained by other investigators. Hamblin does not consider the z_0 estimate to be at all reliable, but fortunately the dependence of ζ on z_0 is small: see Miles (1960, figure 2).

2.2.3. *The power spectrum*

On the basis of the interpretation of the Miles–Phillips theory given by Phillips & Katz we can predict the frequency of the peak of the power spectrum, or, more precisely, that of the rapid rise in the spectral density. This was estimated using the formula $F_T = \lambda_T/2\pi\zeta$, in which ζ was obtained from Miles (1960) using the logarithmic profile parameters $U_1 = 0{\cdot}6$ m/sec and $z_0 = 0{\cdot}1$ mm. The results for the relevant frequencies are given in table 1. The actual upwind fetch available is 6300 m. This intersects the $F_T \times f$ curve at $f = 0{\cdot}52$ cycles/sec, which is the predicted transition frequency. Corresponding to a 50 % uncertainty in F_T, the uncertainty in the predicted frequency is $\pm 0{\cdot}05$ cycles/sec.

f (cycles/sec)	F_T (m)
0·4	21,000
0·5	7,400
0·6	3,400

TABLE 1. Transition fetch *vs.* frequency

We may also predict the form of the high-frequency end of the spectrum, since Phillips (1958*b*) has shown dimensionally that it must fall off as f^{-5}. The measurements of Burling (1959) indicate a $-5{\cdot}5$ exponent, while those of Kinsman (1960), made at longer fetches, follow a $-4{\cdot}5$ power law. We therefore predict a variation approximately as f^{-5}; on the basis of the empirical evidence, we expect this form to be exhibited from the peak frequency upwards (though not of course into the ripple range). However, this prediction cannot be derived from the Miles theory, which imposes no limit to the exponential growth.

2.2.4. *The directional spectrum*

(*a*) *The low frequencies.* Below the peak of the spectrum we anticipate resonance waves at azimuths measured from the wind direction of $\pm \cos^{-1}(c/U)$, where c is the wave velocity and U is the convection velocity of the component of the pressure pattern having the corresponding wave-number. Following Lighthill (1962), the latter is identified with the wind speed at a height of $0{\cdot}25\,\lambda$ above the surface. The wind speed was actually measured at a fixed height, 2 m above the surface, but, since the variation with height is small at heights of $0{\cdot}25\lambda$ for the

relatively long waves under consideration, estimates based on the logarithmic profile parameters used in the calculation of the transition frequency are considered sufficiently accurate. The resonance angles are given in table 2 for the actual frequencies at which the data analysis was carried out.

f (cycles/sec)	λ (m)	$U(0{\cdot}25\lambda)$ (m/sec)	c (m/sec)	c/U	$\cos^{-1}(c/U)$ (°)
0·261	23·0	6·45	5·97	0·925	22
0·284	19·4	6·35	5·48	0·867	30
0·310	16·3	6·25	5·05	0·807	36
0·338	13·7	6·15	4·63	0·752	41
0·368	11·5	6·06	4·24	0·703	45
0·401	9·7	5·95	3·81	0·641	50
0·437	8·2	5·82	3·56	0·608	53
0·476	6·9	5·70	3·27	0·575	55

TABLE 2. Resonance angles *vs.* frequency

(*b*) *The higher frequencies.* In calculating the frequency of the rapid rise in the power spectrum we considered only the upwind fetch and, by implication, waves travelling with the wind. Actually F_T is a function of vector wave-number, and the expression for ζ involves the angle α between the direction of wave propagation and that of the wind; α was taken to be zero in the earlier calculation. Using the vector form of F_T we can compute the transition fetch for waves travelling in any direction and, by comparison with the fetch actually available in that direction, we can estimate for waves of any frequency the azimuths over which transition should have occurred according to the theory. The theoretical fetch required for transition was calculated as a function of azimuth for the frequencies at which the measurements were analysed. Curves of 'fetch required' are plotted in figure 3 along with the curve of 'fetch available', replotted from figure 2. For a fixed frequency the azimuths between the points of intersection of the two curves give the range over which high spectral values are to be expected. If θ_1 and θ_2 are the points of intersection, we define the mean direction of travel to be $\bar{\theta} = \frac{1}{2}(\theta_1 + \theta_2)$ and the angular width of the spectrum as $\Delta\theta = (\theta_2 - \theta_1)$. Values of $\bar{\theta}$ and $\Delta\theta$ are plotted against frequency in figures 4 and 5, and these curves constitute the theoretical prediction for the directional spectrum at the higher frequencies.

Values of θ_1 and θ_2 obtained from figure 3 are given in table 3, along with the derived quantities $\bar{\theta}$ and $\Delta\theta$. Angles are in array co-ordinates.

	f (cycles/sec)											
	0·500	0·520	0·566	0·618	0·674	0·735	0·802	0·875	0·954	1·04	1·135	1·24
θ_1	78	72	69	66	59	55	50	42	35	27	22	18
θ_2	80	91	107	119	123	127	131	134	136	138	141	143
$\bar{\theta}$	79	82	88	93	91	91	91	88	86	83	82	81
$\Delta\theta$	2	19	38	53	64	72	81	92	101	111	119	125

TABLE 3. Mean wave direction and angular spread

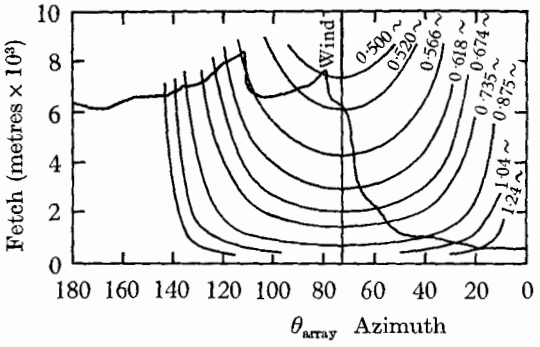

FIGURE 3. Fetch available and calculated fetch required for transition. The symbol ~ used on the figure stands for cycles/sec.

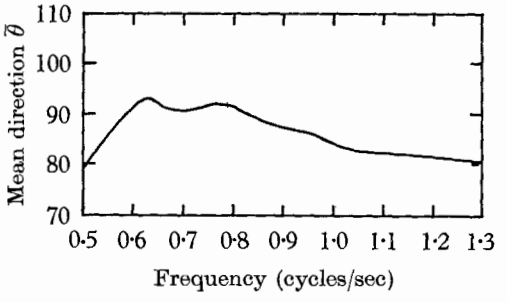

FIGURE 4. Predicted mean direction of propagation—Miles régime.

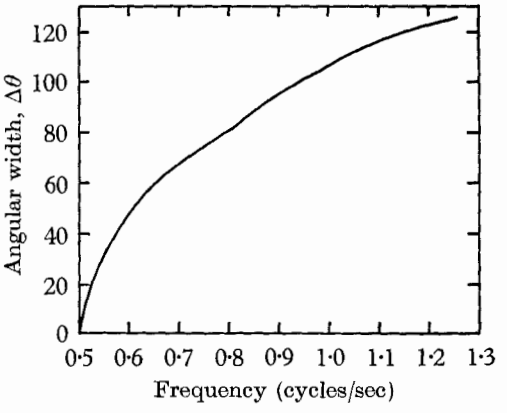

FIGURE 5. Predicted angular width of spectrum—Miles régime.

2.3. *Method of deducing the directional spectrum from array data*

The co-spectra and quadrature spectra of the recorded signals were obtained, using an analogue computer, for each of the 18 separations nD, $n = 0, 1, 2, \ldots, 17$, of detector pairs presented by the array, and for each of 20 frequencies. These functions are denoted by $C_n(f)$, $Q_n(f)$. The directional spectrum $E(\theta,f)$ was obtained from the C and Q by the Fourier–Bessel method described by Barber

(1959). Barber shows that, if $E(\theta,f)$ is expressed as a Fourier series in θ:

$$E(\theta,f) = \sum_{r=0}^{\infty} (A_r \cos r\theta + B_r \sin r\theta),$$

the coefficients A_r, B_r are related to the co- and quad-spectra as follows:

$$C_n(f) - iQ_n(f) = 2\pi \sum_{r=0}^{\infty} i^r (A_r \cos r\theta_n + B_r \sin r\theta_n) J_r(2\pi k D_n), \tag{5}$$

where D_n is the separation of the nth pair of detectors, and θ_n the direction of the line joining them. The directional spectrum $E(\theta,f)$ for a given frequency may thus be found if we can evaluate the coefficients A_r, B_r in this relation.

For each n, that is for each separation presented by the array, we have one equation, but the number of the unknowns A_r, B_r is infinite. However, for a fixed z the value of $J_r(z)$ decreases rapidly with increase of r after a certain value of r, so that the coefficients of the higher A_r, B_r approach zero. It appears reasonable therefore to truncate the infinite series at some $r = R$ and to solve the resulting set of equations for A_r, B_r for $0 \leqslant r \leqslant R$. In order to obtain estimates of A_r, B_r which are stable with respect to variation of R, a rectangular lag window was used. The method was as follows: to the set of 18 equations having measured values of C and Q as their left-hand sides was adjoined a further set, corresponding to greater separations, and the left-hand sides of these were set equal to zero. This augmented set was solved by a regression technique for various values of R. The value of R finally adopted, i.e. the point at which the infinite series was truncated, was selected so that the estimates of A_r, B_r were stable and such that $E(\theta,f)$ contained only significant terms, as decided by the resolving power of the array. The spectrum thus obtained in terms of its Fourier coefficients was smoothed by taking the Cesaro partial sum of the series rather than the ordinary Fourier partial sum. As a check on the method, the spectrum was recalculated for a few frequencies using the Fourier transform method; the agreement was found to be good.

3. Experiment

3.1. *Apparatus*

The experiment was conducted at the IOUBC research station in Burrard Inlet. A map of the site is shown in figure 1. The station consists of a platform about 5 m square mounted on piles about 7 m above the bottom, with a hut to house the equipment and personnel. The measurements for the directional spectrum were made using a linear array of seven wave detectors, which was suspended from cantilever beams attached to the platform structure, and which could be raised out of the water when not in use. The wave detectors were of the capacitance type with teflon dielectric, the capacitance of which varied with changes in water level. The variable capacitance was used as a frequency-determining element in a Wien bridge oscillator. The FM signals from the oscillators were transmitted to the hut by coaxial cables, where they were recorded on magnetic tape.

Calculations described in § 2 indicated that the required partially developed sea would exist with easterly winds of 4–8 m/sec. For a wind of 6 m/sec, in the

centre of this range, the calculated frequency of the peak of the power spectrum was 0·5 cycles/sec; the design frequency range was therefore taken to be 0·25–1·0 cycles/sec, an octave on either side of the peak frequency. In terms of wavelength, the design range was 1–25 m. The expected wave height was obtained from rough visual observations at the site, and was of the order of half a metre. Since the IOUBC station is built on a sandbank with a maximum water depth of 4 m at high tides, it was planned to take measurements at high tides only, in order to minimize depth effects on the waves, and because the currents are then small or zero.

The wave probe consisted of a $\frac{1}{4}$ in. (0·6 cm) diameter brass rod covered with teflon tubing of 0·015 in. (0·037 cm) wall thickness, sealed at the bottom and with an electrical connexion at the top leading to the Wien bridge oscillator. The calculated capacitance of the probe was 6 pF/cm. From the expression for the frequency of the Wien bridge oscillator, the theoretical sensitivity of the wave detector was found to be $S = 3f/C$ cycles $\mathrm{sec}^{-1}\,\mathrm{cm}^{-1}$, where f is the centre frequency of the oscillator and C is the total capacitance in the series arm of the bridge—the sum of the capacitance of the probe, probe cable, and any additional loading capacitance used. If changes of surface elevation of the order of 1 mm are to be detectable, the sensitivity must be about 10 cycles $\mathrm{sec}^{-1}\,\mathrm{cm}^{-1}$; greater values lead to poor linearity characteristics, so that $S = 10$ cycles $\mathrm{sec}^{-1}\,\mathrm{cm}^{-1}$ was used for design purposes. The detector was calibrated by measuring the oscillator frequency for various depths of probe immersion in a tank; the calibration was checked after installation in the array, exploiting the rising tide to give varying depths of probe immersion.

The array was designed as an optimum linear array of seven detectors as defined by Barber (1958). The intervals between adjacent detectors were in the ratio 1:1:4:4:4:3. If the unit interval is denoted by D, the diffraction pattern of the array is given by

$$G(l) = (\sin 35\pi lD)/(\sin \pi lD), \tag{6}$$

where l is the component of wave-number along the line of the array. If a single sharply defined train of waves of unit energy is incident normally on the array, $G(l)$ gives the energy distribution as a function of wave-number which the array will record. The half-power points of the central maximum of $G(l)$ correspond to directions of travel differing by the angle (in radians)

$$\Delta\theta = 0{\cdot}0345\lambda/D,$$

which may be taken as a measure of the resolving power of the array. While, as we have seen, the true power density associated with any azimuth appears to be spread over the entire azimuth circle according to $G(l)$, the spreading is mainly confined to the angle $\frac{1}{2}\Delta\theta$ on either side of the true azimuth. We have estimated the wavelength range of interest to be $1 \leqslant \lambda \leqslant 25$ m, with the spectral peak at $\lambda = 6$ m, and this, together with the expression for $\Delta\theta$, makes it possible to select the unit space D of the array on a logical basis. The value chosen was $D = 0{\cdot}5$ m, which is smaller than would have been selected on the basis of resolution alone, but the choice was further restricted by considerations of the manageability of

a large array. Actually the expression for $\Delta\theta$ indicates that resolving power improves indefinitely with increasing D, but this is not so. In the first place the correlation between the signals from two detectors 'runs out' in about $1\frac{1}{2}$ wavelengths for detectors arranged transversely to the wind direction—i.e. the correlation becomes so small that it is lost in the noise. Secondly, the unit space D must not be greater than half the wavelength of the shortest waves which it is desired to study, since otherwise ambiguities arise in interpreting the measurements. The value adopted enabled measurements to be made down to a lower wavelength limit of 1 m.

Wind speed was measured by a Casella 3-cup anemometer, which was mounted on one end of the top member of the probe frame, with the cups half a metre above the top of the frame, and 2 m above the water surface when the frame was in position for making measurements. The anemometer was thus well removed from any obstruction to the airflow. Wind direction was obtained from a Casella vane of the distant reading type. A Savonius rotor-type meter was used at first to measure current speed and direction, but, since the condition of interest was at near-zero current speeds, it was found more accurate to time the passage of a piece of paper in the water, just below the surface, between the pilings of the IOUBC station.

3.2. *Operation*

Data runs required the following conditions: wind from the east, with speeds in the range of 4–8 m/sec; high tide, with zero current, within about 10 cm/sec; no ship waves or swell present. It was also found advisable to take data only in light rain, although this was more usual than not, with east winds in the winter months when the records were taken. This requirement was added because of a phenomenon encountered earlier. It was found that under some conditions the teflon insulation of the probes was wetted by the water, which, instead of following the wave profile, adhered to the teflon in a thin film which could be observed by the eye. When the water was clean, as judged visually, and by the presence of small capillary waves, no film could be seen. At other times the film could be seen extending up the probe as far as the highest previous wave crest, and it drained very slowly. Under these conditions the oscillator signal was not modulated, so that the waves were not recorded. Now similar probes had previously been used successfully at the same location, and the principal difference in the circumstances appeared to be the fact that they had been used under west-wind conditions, while in this investigation they were used in east winds; it seemed reasonable to suppose that the difference was due to contaminants carried out of Vancouver harbour when the wind blew from the east. It was observed that visually clean water seemed to be associated with the occurrence of rain and wave breaking. The facts were consistent with the supposition that a surface film on the sea, probably more in the nature of a tenuous dispersion of organic molecules than a uniform monolayer, was responsible for the malfunctioning of the detectors. On this basis the action of rain or of wave breaking could be explained as having the effect of driving the surface film into solution. This hypothesis was suggested by Dr R. W. Stewart of IOUBC. Some further evidence was found by Dr R. W. Burling, also of IOUBC, who discovered that a similar wave detector, using a

blocking oscillator in place of the Wien bridge type, continued to operate in conditions where the latter failed completely, even using the same capacitance probe. The apparent differences between the two oscillators were in the d.c. bias applied to the probe, the size of the a.c. voltage swing across the probe, and the waveform—that of the blocking oscillator containing very much higher frequency components, for which the film resistance would be greater as a result of skin effect. The physical and chemical mechanisms of this fouling phenomenon were not investigated further, since the conditions under which fouling occurred could readily be avoided.

At the start of a data run, the probes were first carefully cleaned with moistened paper towels. The probe frame was then lowered into the water, and the height adjusted so that the probes were immersed to a depth of about half a metre, using the pulley blocks by which the frame was suspended. The frame was next run out to the end of the cantilevers on steel tracks, and the bracing ropes secured. The oscillators were then started and the signals switched to separate direct record channels of the Ampex tape recorder. During the run the performance of the wave detectors was monitored by playing back the signals from the tape recorder through demodulators, and displaying the demodulated outputs on a paper recorder.

The most difficult condition to satisfy was the requirement that ship waves be absent. One run, however, was made in ideal circumstances, with no ships in sight during the entire run. The best section of this run, as determined primarily by the zero-current condition, was selected for detailed analysis.

4. Results

The results of the analysis of the wave-detector array records are presented in figures 6–8. Figure 6 is the power spectrum shown on a linear plot, and figure 7 gives the same information in log–log form. Figure 8 is the directional spectrum $E(\theta,f)$ plotted against azimuth for the frequencies at which the analysis was carried out.

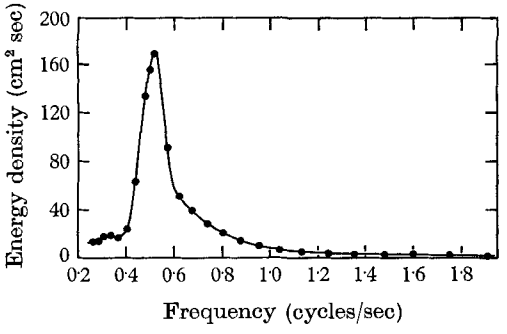

FIGURE 6. Wave power spectrum.

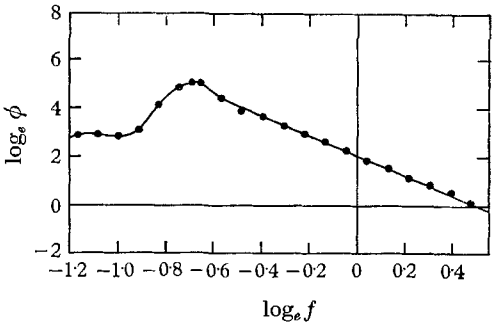

FIGURE 7. Wave power spectrum—log–log plot.

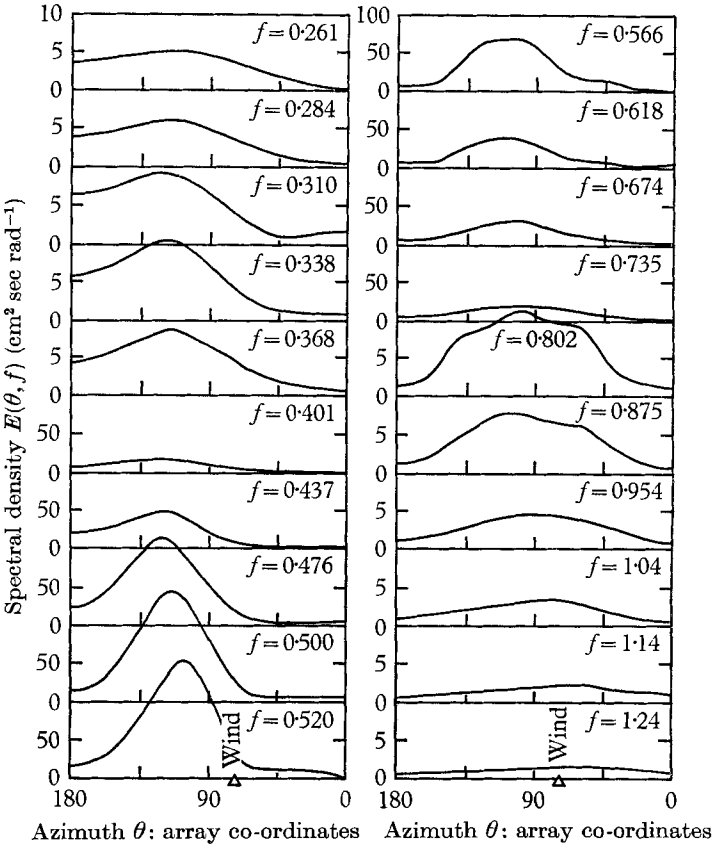

FIGURE 8. Directional spectrum.

5. Discussion of results

5.1. *The power spectrum*

The power spectrum of the water surface displacement is presented in figure 6. For the purposes of this investigation, the feature of greatest interest in the power spectrum is the frequency at which it peaks, for which a theoretical estimate was obtained in § 2.2.3. This estimate was based on a model in which the spectrum rises very rapidly to a peak, from the low levels characteristic of the low frequencies, and really applies to the frequency of this rapid rise rather than the peak. The rise of the measured spectrum is not so abrupt, although this is probably due in part to the finite bandwidth of the filters. Allowing for this effect, we may take the measured values as indicating a rapid rise at $f = 0{\cdot}48$ cycles/sec, and the peak frequency is 0·52 cycles/sec. The predicted value for the frequency of the rapid rise was $f = 0{\cdot}52 \pm 0{\cdot}05$ cycles/sec, which agrees well with the measurements. The agreement is actually somewhat better than this, for the prediction was based on the upwind fetch, whereas from figure 3 we see that transition should first occur, according to the theory, for waves travelling about 6° off the wind, and the transition frequency is more accurately estimated at

$f = 0{\cdot}50$ cycles/sec. Although the central interest in this investigation is in the directional spectrum, the theoretical predictions for the latter, at least in the Miles régime, depend upon an extension of the argument used in predicting the peak of the power spectrum. The excellent agreement obtained in this case therefore increases our confidence in the predictions for the directional spectrum.

As a matter of secondary interest we may determine the best-fitting power law, $\phi(f) = Af^n$, for the high-frequency part of the power spectrum. The spectrum is replotted in log–log form in figure 7, from which we estimate the values of the parameters to be $A = 7{\cdot}9\,\mathrm{cm}^2\,\mathrm{sec}$, $n = -4{\cdot}2$. These values agree reasonably well with earlier measurements.

5.2. *The directional spectrum*

The characteristics of the directional spectrum are discussed separately for the Miles régime (frequencies above that of the peak of the power spectrum) and for the Phillips régime (frequencies below that of the peak of the power spectrum).

5.2.1. *The Miles régime*

The principal characteristics of the directional spectrum to be expected on the basis of the theory were presented in § 2.2.4. For the Miles régime the prediction gave the variation with frequency of the mean direction of wave travel, and of the angular spread of the waves. It will be recalled that these quantities were defined in terms of the angles θ_1 and θ_2, the azimuths between which high spectral values were predicted. In order to compare the theoretical predictions with the results of measurement, we identify θ_1 and θ_2 with the azimuths of the half-power points of the measured spectra, i.e. with the azimuths at which the spectral density has half its peak value for the frequency concerned. In table 4 these values, together with the mean direction of travel $\bar{\theta} = \frac{1}{2}(\theta_1 + \theta_2)$, and the angular width of the spectrum $\Delta\theta = (\theta_2 - \theta_1)$, are tabulated using array co-ordinates.

	f (cycles/sec)											
	0·500	0·520	0·566	0·618	0·674	0·735	0·802	0·875	0·954	1·04	1·14	1·24
θ_1	86	82	77	78	74	52	47	41	30	37	12	10
θ_2	142	136	141	142	142	146	147	145	148	147	138	130
$\bar{\theta}$	114	109	109	110	108	99	97	93	89	92	75	70
$\Delta\theta$	56	54	64	64	68	94	100	104	118	110	126	120

TABLE 4. Experimental values of $\bar{\theta}$ and $\Delta\theta$

In figures 9 and 10, the experimental values of $\bar{\theta}$ and $\Delta\theta$ are compared graphically with the theoretical predictions. A scale of wind co-ordinates is given in figure 9 to emphasize the difference between the mean direction of travel of the waves, and the wind direction.

The first conclusion to be drawn from figure 9 is that the direction of wave travel is indeed displaced from the wind direction in the sense predicted by the theory. Further, the amount of the displacement is in order-of-magnitude agreement with the predictions. Although the definitions adopted for the angles θ_1 and

θ_2 are somewhat arbitrary, it is easily seen by inspection of the directional spectra that the value of $\bar{\theta}$ is affected only slightly by any reasonable definitions of these angles.

The quantitative agreement of the theoretical and observed mean directions is good over the middle frequencies of this range. The results for the highest three frequencies are probably becoming unreliable, since the wave energy is very small. The experimental points are scattered on both sides of the theoretical curve, so that we may consider the results as confirming the theory for the high frequencies also.

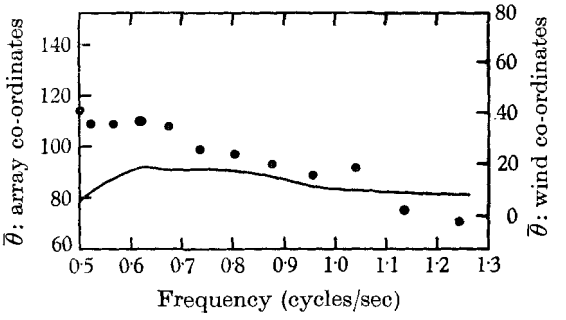

FIGURE 9. Mean direction of wave propagation.

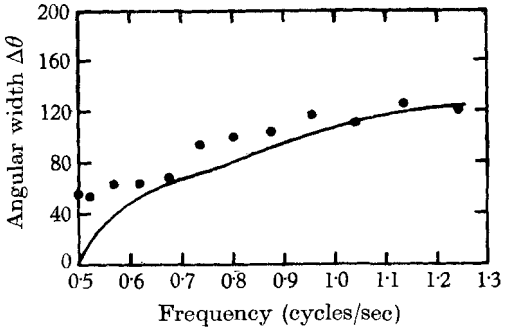

FIGURE 10. Angular width of spectrum.

The discrepancy between the measurements and the predictions is greatest at the lower end of the frequency range, and it increases with decreasing frequency. The following argument is offered as a possible explanation. Although at these frequencies the Miles mechanism is strongly operative, it may not have obliterated all traces of the resonance waves. But there is reason to suppose that the resonance wave approaching from north of the array normal has much greater energy than that from the south; this will be explained in § 5.2.2. Effectively, therefore, the resonance waves are displaced from the wind direction in the same sense as Miles waves, and at the frequencies concerned they are displaced to a greater extent. The resultant effect would be an increase in the net displacement, as observed. This possibility is supported by the fact that the angle θ_1 is in fairly good agreement with the predicted value, and the discrepancy in $\bar{\theta}$ arises mainly because θ_2 is greater than the theory indicates. The effect suggested is not amenable to treatment by the existing theories.

Another effect arises from the variability of the wind direction, and the irregularity of the fetch. The wind direction was observed to vary by $\pm 10°$ about the mean direction. Normally, with a symmetrical fetch, variation of wind direction would not be expected to influence the mean direction of wave travel. The effect in the present case is most easily understood by an examination of figure 3, considering the result of a translation in azimuth of the U-shaped curves relative to the geometric fetch curve. For a variation of $\pm 10°$ the maximum displacement is 2°, at a frequency of 0·566 cycles/sec. This effect is small, but it has the sense required to account for the discrepancy, and it occurs in the frequency range where the discrepancy is greatest.

The angular spread results are shown in figure 10, from which it is seen that the observed values agree fairly well with the theory, both in order of magnitude and frequency trend. In this case the magnitude does depend considerably on the definitions adopted for θ_1 and θ_2, and exact agreement is hardly to be expected. The greatest discrepancy is again at the low end of the frequency range. The greater observed spread at these frequencies is consistent with the argument that residual resonance waves are present. The effect of wind direction variability would of course be to increase the observed angular spread; although the observed spread angles do lie above the theoretical curve, no definite conclusions should be drawn from this fact in view of the arbitrary definitions of θ_1 and θ_2.

5.2.2. *The Phillips régime*

According to the theoretical considerations of § 2.1, the wave energy at the low frequencies should be concentrated around two azimuths equally displaced from the wind direction. The displacement is given by Phillips's resonance angle, $\pm \cos^{-1}(c/U)$, the values of which are tabulated for each frequency analysed, in § 2.2.4.

The directional spectra for these frequencies do not exhibit the bimodal characteristic that would be expected according to a straightforward application of the theory. We shall return to this point later, but first let us consider the mean direction of travel of the waves actually observed. The azimuth of the maximum spectral density is probably the most appropriate measure in this case, although the choice is not critical. The experimental values are given in table 5 together with the theoretical angles for resonance waves from § 2.2.4; to facilitate comparison, the experimental angles are quoted in wind co-ordinates. Agreement would not be expected for the highest two frequencies, since as can be seen from the power spectrum the Miles mechanism is acting in these cases; the highest frequency in fact represents the peak of the power spectrum. But what can be said as regards the rest of the range? The order of magnitude is certainly correct, but the frequency trend of the experimental results—if indeed a trend exists—does not agree at all well.

f (cycles/sec)	0·261	0·284	0·310	0·338	0·368	0·401	0·437	0·476	0·500	0·520
$\bar{\theta}_{\text{expt.}}$	41	45	46	45	44	48	49	48	40	32
$\cos^{-1}(c/U)$	22°	30°	36°	41°	45°	50°	53°	55°	—	—

TABLE 5. Experimental values of $\bar{\theta}$

However, we have so far ignored the fact that waves of the frequencies involved are not effectively deep-water waves for the last part of their travel, as they traverse the sandbank on which the IOUBC experimental station is located, so that the waves will be refracted. The sandbank is shown shaded in figure 1: a larger scale map of the bank is shown in figure 11, from which it may be seen that the edge of the bank can be represented quite well by two straight lines. For all directions of travel under consideration the waves will cross the edge of the bank where the latter bears 13° south of east. The bottom contours are such that this line may be considered to divide the fetch into a deep water region north and east of the line, and a shallow water region of uniform depth from the line to the measuring site. The depth in the shallow region at the time of the measurements was 3 metres. In this simple situation it is possible to estimate the refraction effect quite accurately.

The problem is to find the direction of travel of the incident wave over most of the fetch, where the water is deep. The geometry of the idealized model is given in figure 12. If the wave phase speed in deep water is c_0, and in a depth of 3 m is c, the simple refraction formula gives

$$\cos\phi_0/\cos\phi = c_0/c = \lambda_0/\lambda = \coth(2\pi h/\lambda), \tag{7}$$

where h is the water depth, and λ the wavelength in the shallow region; the suffix zero indicates deep-water quantities, and the angles ϕ and ϕ_0 are defined by figure 12. To avoid iteration, let $u = 2\pi h/\lambda$, and $A = 4\pi^2 hf^2/g$; then $\cos\phi_0/\cos\phi = u/A$, where u is the solution of $A = u\tanh u$, which is easily found graphically. From figure 12, $\phi = \bar{\theta}+1$, and hence $\phi_0 = \cos^{-1}\{(u/A)\cos(\bar{\theta}+1)\}$. The angle we wish to find is $\bar{\theta}_0$, the angle between the wind direction and the direction of travel of the wave in deep water. From the figure this is seen to be

$$\begin{aligned}\bar{\theta}_0 &= \bar{\theta}+(\phi_0-\phi) = \phi_0-1,\\ &= [\cos^{-1}\{(u/A)\cos(\bar{\theta}+1)\}-1].\end{aligned} \tag{8}$$

The mean directions of travel, corrected for refraction effects according to equation (8), are given in table 6.

f (cycles/sec)	0·261	0·284	0·310	0·338	0·368	0·401	0·437	0·476	0·500	0·520
u/A	1·268	1·202	1·142	1·094	1·060	1·032	1·013	1·003	1·000	1·000
$\bar{\theta}$	41°	45°	46°	45°	44°	48°	49°	48°	40°	32°
$\bar{\theta}_0$	18°	33°	38°	40°	41°	47°	48°	48°	40°	32°
$\cos^{-1}(c/U)$	22°	30°	36°	41°	45°	50°	53°	55°	—	—

TABLE 6. Corrected values $\bar{\theta}_0$

As expected, the effect of refraction is small for the higher frequencies in this range, but becomes appreciable at the lower frequencies. The net effect is to give much better agreement between the experimental results and the theoretical resonance angle, particularly in regard to the frequency trend. The comparison is shown graphically in figure 13. The agreement is such that one can scarcely avoid the conclusion that the observed waves represent one of the two trains

predicted in the Phillips theory, especially as it would be difficult to account for the results on any other basis. However, if this is so, what has happened to the other wave train?

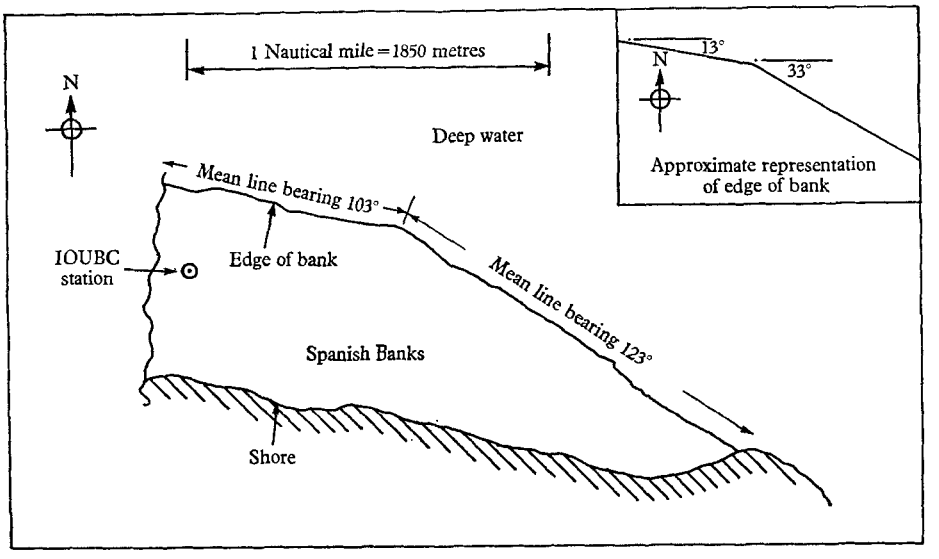

FIGURE 11. Map of Spanish Banks.

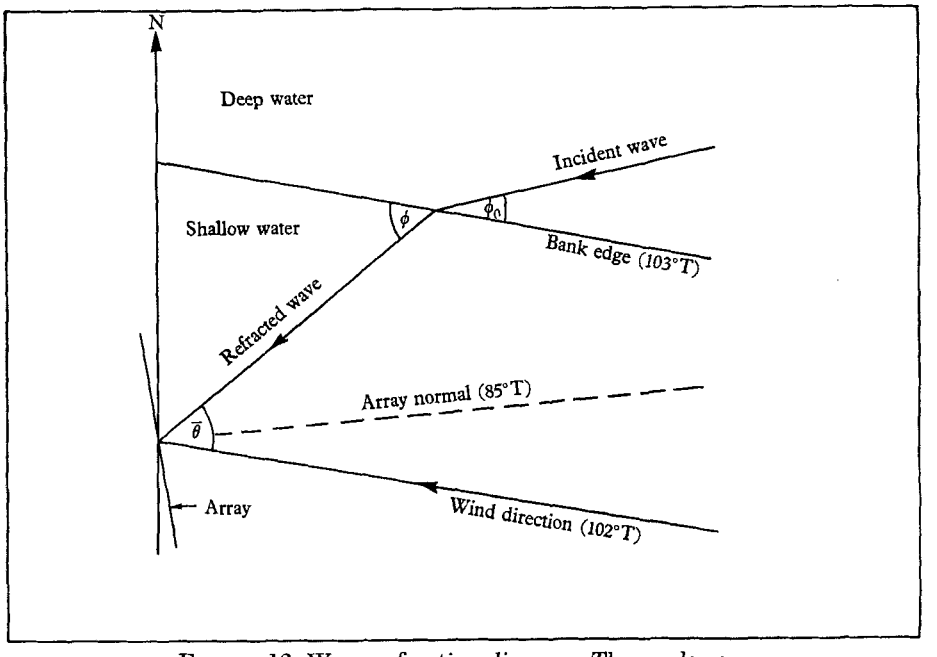

FIGURE 12. Wave-refraction diagram. The angles are given relative to true north (°T).

The first part of the answer to this question is to be found from an examination of figure 2. The observed waves approach the array from directions to the north of the wind direction, where the available fetch is about 8 km. Waves coming

from directions equally inclined to the wind, but to the south of the wind direction, have a fetch of only about 1 km. Now from § 2.1 the spectral density of waves in the Phillips régime increases linearly with the wind duration or, equivalently, with the fetch. Hence we would expect the second spectral peak to be much lower than the first, of the order of 12 %, on the basis of the asymmetry of the fetch. But the waves corresponding to this hypothetical second peak travel in shallow water over their entire fetch, and moreover, the depth decreases in an irregular way towards the shore. As a result the waves experience continuous

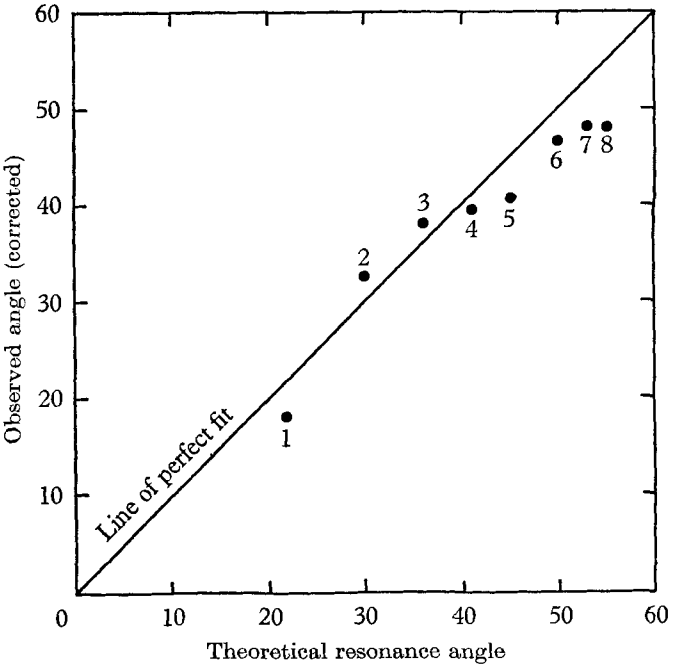

FIGURE 13. Goodness-of-fit diagram.

Point	Frequency (cycles/sec)	Point	Frequency (cycles/sec)
1	0·261	5	0·368
2	0·284	6	0·401
3	0·310	7	0·437
4	0·338	8	0·476

variation in wavelength and speed of travel, and in direction of travel also, because of refraction. But the resonant response of Phillips's mechanism depends upon the waves remaining in step with the forcing pressure pattern. If, for some wave-number component of the pattern and some free wave, the necessary condition $U\cos\theta = c$ holds at a given instant, and if θ, c, and λ then change arbitrarily, as dictated by the bottom topography, the condition will no longer be satisfied and so the wave cannot continue to grow resonantly. Actually, if the fetch were divided into regions of approximately constant depth, we might expect that in each region resonance waves of a given frequency would start to grow, each with a different direction of travel. Each wave would cease to grow as

it passed out of the region in which it was formed, but it would continue to suffer refraction. The total energy of this frequency observed at the measuring site would be the total energy of the waves from each region, each with its own refracted direction of travel, plus the energy of the forced waves. Since the theory predicts a linear rate of energy growth, the integral over azimuth of the energy of the waves coming from south of the wind direction might be expected to be of the order of 12 % of that for waves from the north, as estimated on the basis of the fetch. Because of refraction and the different directions of travel as generated, the observed energy would be spread out in azimuth, and, especially for the lower frequencies, would tend to concentrate near the array normal, which is roughly parallel to the contour lines, and so would be lost in the tail of the first spectral peak. In other words this argument suggests that no second peak should be discernible under the conditions of the experiment.

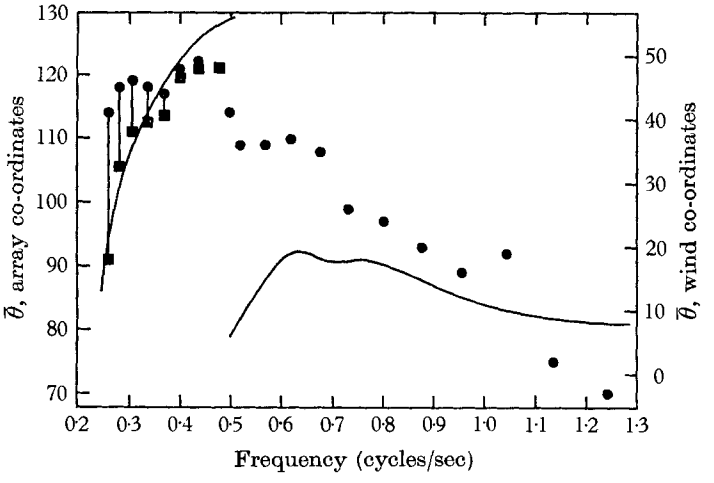

FIGURE 14. Comparison of theoretical and experimental direction of propagation. ●, Experimental results; ■, experimental results with refraction correction.

If this argument is correct it disposes of the principal obstacle to the identification of the observed waves as one of the trains predicted by Phillips, and the good agreement in magnitude and frequency trend, and especially the sudden jump in the off-wind angle below the frequency of the spectral peak constitutes strong evidence for the validity of Phillips's theory. It would however be very desirable to repeat the experiment under conditions of symmetrical fetch and in deep water, since observation of the bimodal spectrum would be the most convincing proof of the theory. Another investigator at IOUBC plans to make such measurements in the near future.

The experimental and theoretical values of $\bar{\theta}$ for both the Miles and Phillips régimes are brought together in figure 14, primarily to illustrate the jump in the off-wind angle at the frequency where the dominant mechanism changes. The jump is a notable feature of the experimental results, but it occurs less abruptly than a simple application of the theory would predict. Evidently, as already

suggested in § 5.2.1, there is a band of frequencies centred on the theoretical transition frequency (0.50 cycles/sec) in which the effects of both mechanisms may be seen.

This work was supported by the Defence Research Board of Canada, Grant No. 9550-09, and was performed while the author was on leave of absence from the Defence Research Board. The assistance of Drs R. W. Stewart and R. W. Burling of IOUBC, in the form of discussions of the work throughout its course, is gratefully acknowledged.

REFERENCES

BARBER, N. F. 1958 Optimum arrays for direction finding. *N.Z. J. Sci.* **1**, 35–51.

BARBER, N. F. 1959 A proposed method of surveying the wave state of the open ocean. *N.Z. J. Sci.* **2**, 99–108.

BENJAMIN, T. B. 1959 Shearing flow over a wavy boundary. *J. Fluid Mech.* **6**, 161–205.

BURLING, R. W. 1959 The spectrum of waves at short fetches. *Dt. Hydrogr. Z.* **12**, 45–64, 96–117.

CONTE, S. D. & MILES, J. W. 1959 On the numerical integration of the Orr–Sommerfeld equation. *J. Soc. Indust. Appl. Math.*, **7**, no. 4.

HAMBLIN, P. 1965 Cup anemometer wind observations over the sea. M.Sc. dissertation, University of British Columbia.

KINSMAN, B. 1960 Surface waves at short fetch and low wind speed. *Tech. Rep.* no. 19, Chesapeake Bay Institute.

KINSMAN, B. 1965 *Wind Waves.* New Jersey: Prentice-Hall Inc.

LIGHTHILL, M. J. 1962 Physical interpretation of the mathematical theory of wave generation by wind. *J. Fluid Mech.* **14**, 385–398.

MILES, J. W. 1957 On the generation of surface waves by shear flows. *J. Fluid Mech.* **3**, 185–204.

MILES, J. W. 1960 On the generation of surface waves by turbulent shear flows. *J. Fluid Mech.* **7**, 469–478.

PHILLIPS, O. M. 1957 On the generation of waves by turbulent wind. *J. Fluid Mech.* **2**, 417–445.

PHILLIPS, O. M. 1958*a* Wave generation by turbulent wind over a finite fetch. *Proc. 3rd U.S. Congr. Appl. Mech.*, pp. 785–789.

PHILLIPS, O. M. 1958*b* The equilibrium range in the spectrum of wind-generated ocean waves. *J. Fluid Mech.* **4**, 426–434.

PHILLIPS, O. M. 1960 On the dynamics of unsteady gravity waves of finite amplitude. *J. Fluid Mech.* **9**, 193–217.

PHILLIPS, O. M. & KATZ, E. J. 1961 The low frequency components of the spectrum of wind-generated waves. *J. Mar. Res.* **19**, 57–69.

URSELL, F. 1956 Article in *Surveys in Mechanics*, pp. 216–249. Cambridge University Press.